Wetlands Ecol Manage (2011) 19:409–421
DOI 10.1007/s11273-011-9225-3

ORIGINAL PAPER

A field based statistical approach for validating a remotely sensed mangrove forest classification scheme

John M. Kovacs · Yali Liu · Chunhua Zhang · Francisco Flores-Verdugo · Francisco Flores de Santiago

Received: 26 January 2010 / Accepted: 25 July 2011 / Published online: 7 August 2011

Abstract Amongst the most threatened ecosystems on Earth, mangrove forests are also one of the more difficult to work in due to their growth in mud and open water coastal zones and their dense tangled stems, branches and prop roots. Consequently, there has been an impetus to employ remotely sensed imagery as a means for rapid inventory of these coastal wetlands. To date, the majority of mangrove maps derived from satellite imagery utilize a simple mangrove classification scheme which does not distinguish mangrove species and may not be useful for conservation and management purposes. Although more elaborate satellite based mangrove classification schemes are being developed, given their enhanced complexity they deserve additional justification for end users. The purpose of this study was to statistically examine the appropriateness of one such classification scheme based on an inventory of field data. In January of 2007 and May of 2008, 61 field sample plots were selected in a stratified random fashion based on a previous classification of a degraded mangrove forest of the Isla La Palma (Sinaloa, Mexico) using Landsat TM5 data. Unlike other previous Landsat TM based classifications of this region, which simply identified the mangrove forests as one class, the mangroves were classified (i.e. mapped) according to four conditions; healthy tall, healthy dwarf, poor condition, and dead mangroves. Within each sample plot, all mangroves of diameter of breast height (dbh) greater than 2.5 cm were identified and their height, condition and dbh recorded. An estimated Leaf Area Index (LAI) value also was obtained for each sample and the shortest distance from the center of each sample plot to open flowing water was determined using a geographic information system (GIS) overlay procedure. These data were then used to calculate mean values for the four classes as well as to determine stem densities, basal areas, and the Shannon–Wiener diversity index. In order to assess the appropriateness of this mangrove classification scheme a discriminant analysis approach was then applied to these field data. The results indicate this forest has undergone severe degradation, with

J. M. Kovacs (✉)
Department of Geography, Nipissing University, North Bay, ON P1B 8L7, Canada
e-mail: johnmk@nipissingu.ca

Y. Liu
Department of Mathematics, East Tennessee State University, Johnson City, TN 37614, USA

C. Zhang
Department of Geosciences, East Tennessee State University, Johnson City, TN 37614, USA

F. Flores-Verdugo
Instituto del Ciencias del Mar y Limnología, Universidad Nacional Autónoma de México, 82000 Mazatlán, Sinaloa, Mexico

F. F. de Santiago
Department of Geography, University of Western Ontario, London, ON N6A 5C2, Canada

decreasing mean tree heights, mean dbh and species diversity. In regards to the discriminant analysis procedure, further classification of these field plots and cross-validation based on these significant variables provided high classification accuracy thus validating the appropriateness of the satellite based image classification scheme. Moreover, the discriminant analysis indicated that the estimated LAI, mean height, and mean dbh are significant in the separation of the classification of mangrove forest condition along these field sample plots.

Keywords Mangrove structure · Degradation · Discriminant analysis · Classification · Mexico

Introduction

Mangrove forests are represented by a variety of tree species that once dominated most tropical and subtropical coasts. These forests have provided both important economical and ecological functions. Economically, they have been identified as important genetic reservoirs and have been shown as the supportive element for recreational and commercial fisheries (Walters et al. 2008). Mangroves are also an important tourism resource and a source of raw materials for the chemical industry (Basak et al. 1996). Regardless of their large scale commercial potential, mangroves are particularly important for local peoples, providing a subsistence fishery resource and a source of material for food, firewood, charcoal, furniture and building materials (Ewel et al. 1998). Ecological roles of mangroves include protection from flooding and wave erosion, sediment trapping, water quality improvement, habitat for wildlife both within the forest and in offshore areas, and as crucial exporters of organic matter and nutrients (Ewel et al. 1998; Duke et al. 2007). Given all of their ecological and economical functions, mangrove forests are still amongst the most threatened of global ecosystems (Valiela et al. 2001; Wilkie and Fortuna 2003). Based on rough estimates, it has been reported that a 1.5% annual global loss of mangroves occurred during the 1980s and 1990s, with the global mangrove coverage falling below 15 million ha by 2,000 (Wilkie and Fortuna 2003). As a result, many (Duke et al. 2007) postulate that mangrove forests will soon disappear altogether if these rates are maintained. The principal causes of mangrove forest loss include pressure from anthropogenic activities such as aquaculture, agriculture, urbanization, pollution, and tourism (Barbier and Sathirathai 2004) and from tidal hydrological variations induced by global climate change and/or anthropogenic causes (Xue 1996; Allen et al. 2001). These activities lead to either direct deforestation or alterations to sedimentation rates, nutrient inputs, freshwater inputs or tidal inundation patterns that subsequently affect the distribution and condition of the mangroves (Hogarth 1999; Linneweber and de Lacerda 2002; Walters et al. 2008). Consequently, changes in salinity regimes within mangroves are often observed and have been treated as a primary reason for observed global changes in mangrove structure and species diversity (Ewel et al. 1998; McDonald et al. 2003; Mitsch and Gosselink 2007).

Due to the increasing pressure on mangrove ecosystems, there have been many efforts to inventory local mangrove forest structure and productivity using traditional field techniques (e.g., Ball 1998; Ewel et al. 1998; Cole et al. 1999). However, such studies, based purely on ground measurements, are extremely difficult to conduct and logistically expensive given the problems of accessibility to and movement through these forested wetlands. Therefore, proper mangrove assessments based on field survey alone are extremely challenging if not impossible at regional and national levels. Given the constant threats to mangroves, it is crucial that mangrove inventory endeavors consider mapping the spatial extents and condition of these wetlands at more regular intervals. Consequently, remote sensing techniques, which remotely collect radiative data from ground objects at different spatial and temporal resolutions, have been shown to be powerful tools in evaluating mangrove forest condition and distribution. Over the past decade or so the vast majority of these applications have employed medium spatial resolution (10–30-m pixel resolution) and multispectral imagery (e.g., Landsat and SPOT XS, Long and Skews 1996; Green et al. 1998; Saito et al. 2003; Tong et al. 2004; Rakotomavo and Fromard 2010) which can limit the thematic accuracy of such mapping endeavors. However, the use of higher spatial resolution optical satellite imagery

(e.g., Wang et al. 2004, 2008; Kovacs et al. 2005, 2009), airborne optical data (e.g., Madden et al. 1999; Welch et al. 1999; Krause et al. 2004; Everitt et al. 2010), airborne hyperspectral data (e.g., Held et al. 2003; Hirano et al. 2003), in field laboratory hyperspectral data (e.g., Vaiphasa et al. 2005; Wang and Sousa 2009) and synthetic aperture radar imagery (e.g., Simard et al. 2002; Lucas et al. 2007; Kovacs et al. 2008a) are now being used for improving mapping inventories. The foci of these remote sensing studies are in image classification (e.g., Kovacs et al. 2001; Simard et al. 2002; Tong et al. 2004; Wang et al. 2004), species separation (e.g., Vaiphasa et al. 2005; Wang and Sousa 2009), quantification of foliage and canopy parameters (e.g. Kovacs et al. 2004; Lucas et al. 2007), and change detection (e.g., Rakotomavo and Fromard 2010). At present most remote sensing studies related to mangroves have focused on their spatial extent and have been limited to one class (i.e., mangrove). Even though different parties may use the same classification techniques and satellite imagery there are often conflicting reports on the estimation of mangrove areas. For example in Mexico, there is a 20,000 ha difference between estimations of mangrove areas from 1991 and 1993, based on remote sensing and field surveys, respectively (Wilkie and Fortuna 2003).

In addition to mapping mangrove extents, others have used the same satellite data to extend their mangrove classification scheme from one mangrove class to many in order to incorporate the overall condition of the forests. For example, in their study of the Teacapán-Agua Brava-Las Haciendas estuarine-mangrove complex of the Mexican Pacific, Kovacs et al. (2001) classified this mangrove forest according to several mangrove conditions (e.g., poor condition mangrove, dead mangrove) instead of one simple mangrove class as employed by Berlanga-Robles and Ruiz-Luna (2002) and Fuente and Carrera (2005). All three studies employed Landsat data but a lack of detail regarding the reference data used to test the classification results has resulted in conflicting reports as to the status of this system. However, subsequent studies using higher spatial resolution satellite imagery has confirmed a degraded mangrove system (Kovacs et al. 2004, 2005, 2009). It is thus suggested that further field work based on such mangrove classes should be conducted to validate the choice of the mangrove forest classification schema which are typically based on expert knowledge and spectral information. Additionally, an examination of these field data may assist in providing insight as to the potential environmental factors contributing to the current status of the mangroves. Such information could be beneficial for those regions where historical records of environmental data are lacking or non-existent, which is typical of most mangrove forests.

The aim of this investigation was to propose a technique for linking mangrove fieldwork data with a remotely sensed mangrove classification, thus justifying the results of the image classification as well as suggesting the most probable cause of the mangrove degradation. Specifically, we sampled a degraded mangrove forest of Isla La Palma (Mexican Pacific) and its surroundings based on a previous remote sensing classification that employed a 2007 scene of Landsat Thematic mapper (TM) data (Kovacs et al. 2008b) in order to elucidate its structure and obtain some data on environmental factors that are related to hydrological change. These biological and environmental variables were then used to reclassify these field data in order to confirm these remote sensing classes are appropriate both in the context of spectral classification and ecological monitoring.

Study area

The Teacapán-Agua Brava-Las Haciendas estuarine-mangrove complex (22°09′N, 105°26′W, Mexico) is one of the largest mangrove systems on the Pacific coast of the Americas (Fig. 1). The system contains numerous lagoons, including the very large Laguna Agua Brava and Laguna Agua Grande, and now has two inlets, the natural inlet of Teacapán, and an artificial inlet, opened in 1972, which is known as the Cuautla canal (>15 m depth and >1000 m width at the mouth). Image sequences (Fig. 2) show the mangroves on and around Isla La Palma have undergone considerable degradation. Areas of the dead mangrove (i.e., dead trunks) have increased considerably between 1986 and 2009. In this region of the Teacapán-Agua Brava-Las Haciendas estuarine-mangrove complex, the black mangrove (*Avicennia germinans*) dominates. Large black mangrove can be found just inland along a very thin fringe of mixed mangrove that consists mainly of healthy red

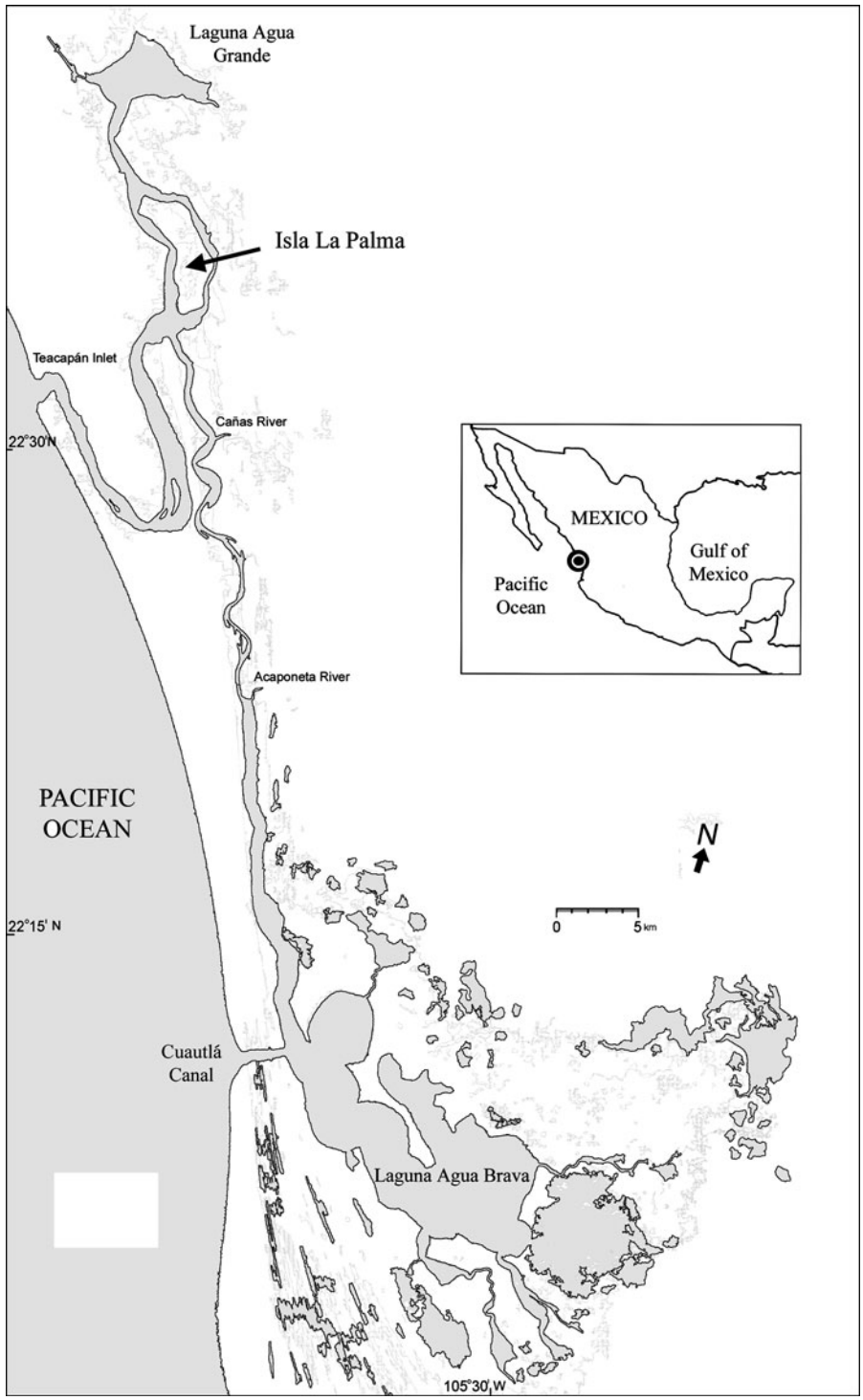

Fig. 1 The Teacapán-Agua Brava-Las Haciendas estuarine-mangrove complex. Please note that there are two inlets to the ocean. The artificial one, the Cuautla canal, is at the south of the study area

mangrove (*Rhizophora mangle*) with some white mangroves (*Laguncularia racemosa*). These mixed mangroves, typically having heights over 7 m and dense green canopies, are located along the edges of the estuaries and islands. Further inland, dwarf black mangrove and poor condition black mangrove are

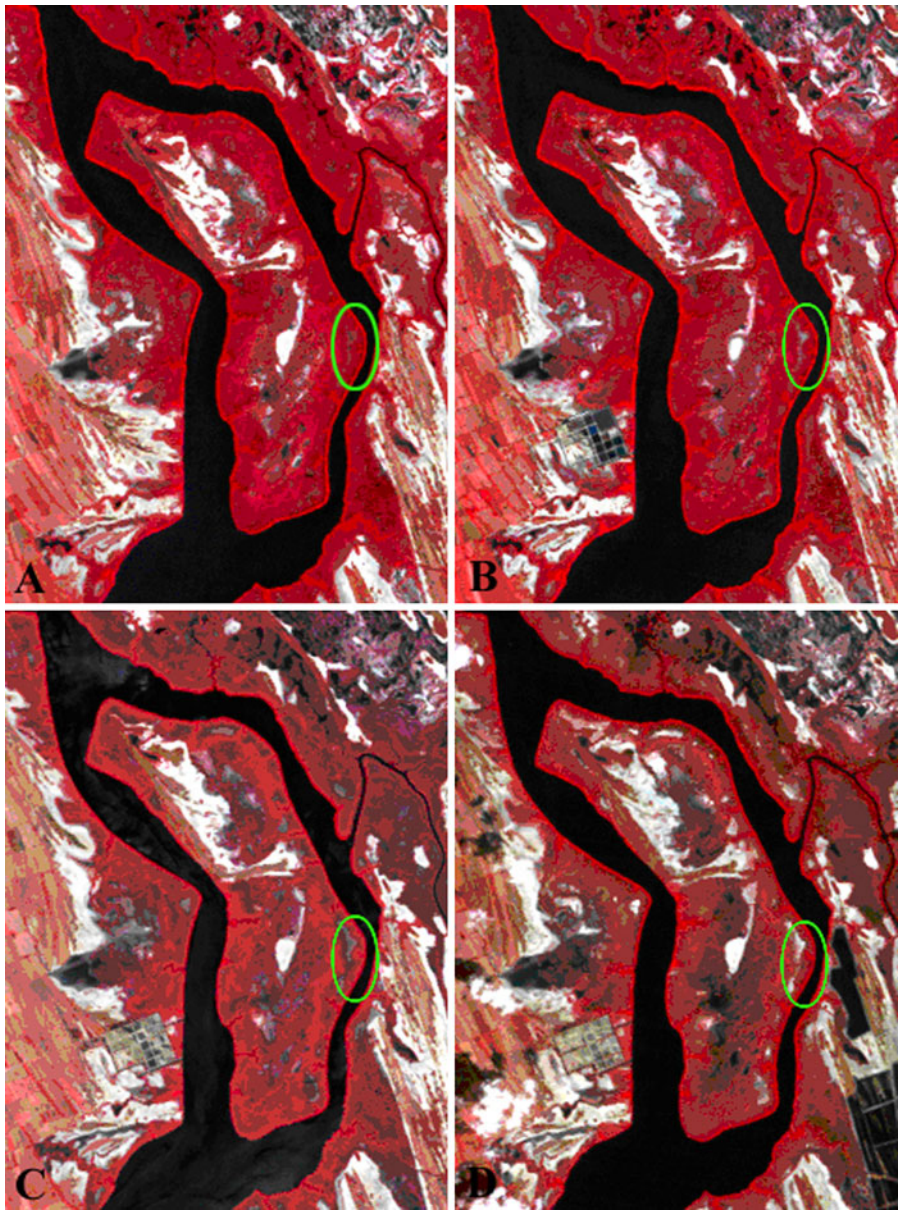

Fig. 2 Degradation of mangrove forest on Isla La Palma. Landsat satellite images are shown in enhanced false color composites. It is clear that the area of dead mangroves has been growing in the last 20 years. Images were taken on: **a** March 10, 1986; **b** February 12, 1994; **c** May 1st, 2005; and **d** March 9, 2009. Areas covered by vegetation are shown as different shades of *red*. Areas with *white* or *bright tone* are saltpans. The *linear red* features along the edge of the shore are fringe (or tidal) mangrove dominated by healthy tall mangroves. Most of the *grey toned* areas on the Isla La Palma represent dead or degraded mangroves. Note the area indicated by the *green circle* which shows a conversion of relatively healthy mangrove to dead mangrove

found (Fig. 3). The poor condition mangrove has a very sparse canopy dominated by yellowish leaves with many dead branches void of leaves. In this type of mangrove, there is a conversion from what was once healthy tall mangrove to a more dwarf type of mangrove, possibly the result of hydrologic changes resulting from the construction of the canal (Kovacs 2000; Kovacs et al. 2001). Many will have a remnant

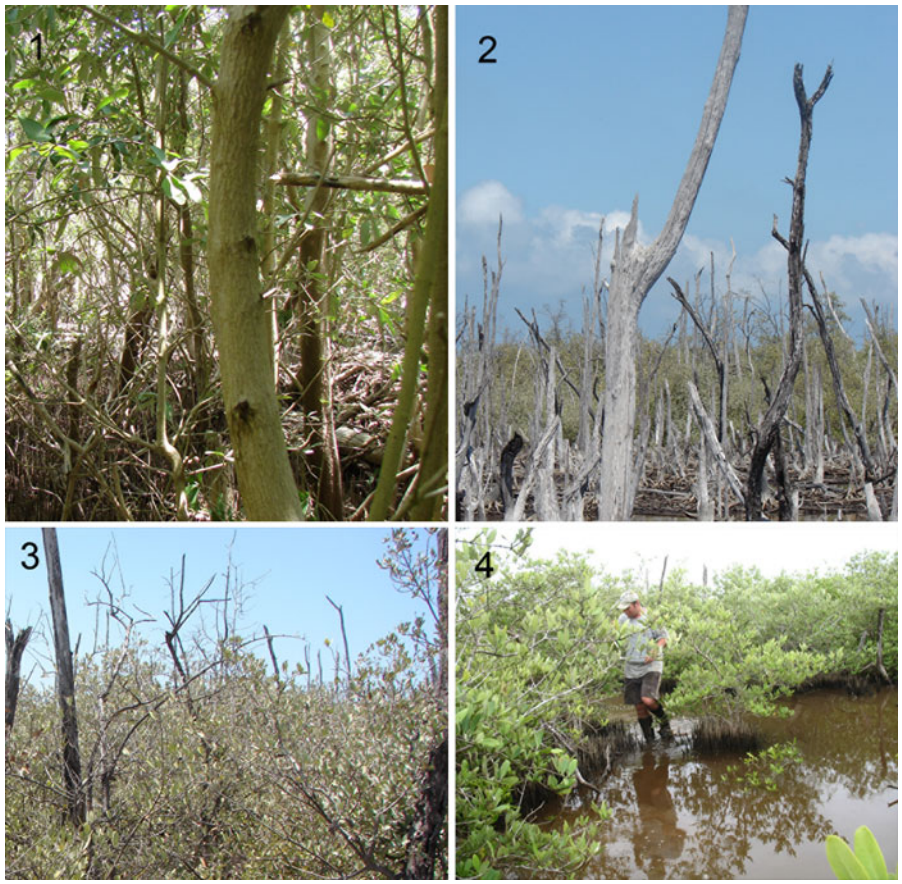

Fig. 3 Examples of the four mangrove classes employed: tall healthy *(1)*, dead *(2)*, poor condition *(3)*, dwarf mangrove *(4)*

tall trunk with only leaves near the base. Dead stands of black mangrove can also be found further inland often bordering salt pans and terrestrial vegetation.

As previously stated there have been efforts to map mangrove conditions for this lagoon based on remote sensing techniques. Kovacs et al. (2001, 2008b, 2009) employed Landsat, ENVISAT Advanced Synthetic Aperture Radar (ASAR) and even QuickBird imagery to map this region in addition to collecting mangrove field data. Kovacs et al. (2001), using Landsat data and a mangrove classification scheme based on the condition of the mangroves, reported that the system was undergoing extensive degradation. Others (Berlanga-Robles and Ruiz-Luna 2002; Fuente and Carrera 2005), using the same type of data but employing a single mangrove class, have reported that the mangroves of the Teacapán region located within the state of Sinaloa, Mexico, had recently expanded.

Methods

Field data collection

A stratified random method using a satellite based mangrove classification scheme was applied in determining field sampling locations. Specifically, the mangroves of this study area had been previously separated (i.e., mapped) according to four conditions (tall healthy, dwarf healthy, poor condition, dead) which had been based on an image classification conducted in 2007 (Kovacs et al. 2008b). The field work was conducted in January 2007 and in May 2008 during local dry season. In total 61 sites were visited.

At each sampling site a circular 0.04 ha field plot (11.3 m radius) was laid out in order to collect information on mangrove stem density, basal area, mean tree height, and mean dbh. Species, dbh, and height were recorded for every tree (including dead

trunks) of greater than 2.5 cm dbh. Tree height information was obtained using a clinometer or, if the tree was short, through simple tape measurement.

The central location of each field plot was identified and recorded using a Trimble GeoXT GPS unit. The raw GPS data were then postprocessed with Trimble Pathfinder software using data obtained from a stationary GeoXT GPS unit (i.e., base station). For consistency and security purposes the base station was secured to the same rooftop location during the two field expeditions and run on continuous mode. The average accuracy of the post processed location data were determined to be at a sub-meter level relative to the base station and processed as UTM based on a NAD 83 projection.

Leaf Area Index (LAI) is a very important canopy structure variable. Data of estimated LAI were obtained from a previous study of this location (Kovacs et al. 2009). Specifically, based on field measured LAI using an Accupar LP-80 Ceptometer, LAI for one scene of QuickBird data (dated April 25, 2007) was calculated using a linear regression technique of LAI as the dependent variable and satellite image digital numbers (DNs) as the independent variable. LAI for each field plot was then obtained using an overlay of plot locations on predicted LAI surface.

It has been hypothesized by many (Flores-Verdugo et al. 1997; Kovacs 2000; Kovacs et al. 2001) that the opening of the Cuautla canal influenced the tidal dynamics in this region and therefore altered the salinity regime. Although this has been suggested as a plausible occurrence by local elders (Kovacs 2000) there are no historical or even current scientific records of salinity to support this. Alternatively, we hypothesize the shortest distance to open flowing water (or freshwater runoff) would be very important in explaining the potential influence of tides on soil pH and water salinity for the mangrove forests. Consequently, the shortest possible distance to open flowing water (i.e., estuary) for each field plot was obtained using ArcGIS. Specifically, based on a QuickBird image and a shapefile of sample location, the shortest distance from the centre of each field plot to open flowing water was recorded.

Data analysis

To show the historical changes of species diversity and structure, a Shannon–Wiener diversity index (H') (Krebs 1989) was calculated for each field plot. The Shannon–Wiener diversity index is defined as $H' = -\sum p_i \ln(p_i)$, where p_i is the proportion of individuals from the ith species. To calculate H', all trees belonging to each condition were combined to calculate the two parameters.

Discriminant analysis was applied to investigate the consistency of remote sensing classes based on expert knowledge and field collected data as it has been widely used to examine the separability of multiple categorical data (e.g., Yu et al. 1999; Salovaara et al. 2005; Wang and Sousa 2009). This technique develops a classification criterion using a measure of generalized squared distance from the mean. Each observation is then classified into a group from which it has the smallest generalized squared distance. Computationally, discriminant analysis is very similar to analysis of variance (ANOVA). When given a group of variables, F tests are conducted to decide which variables are significant to differentiate between groups. Discriminant functions, also known as classification criterion, are developed to assign group membership. Assuming the variance (variance–covariance matrix of the responses) is the same across all classes, this technique results in linear discriminant functions, which is also the maximum likelihood classification approach for traditional pixel based image classification. Alternatively, each class has a unique variance structure and a quadratic discriminant function is produced. A statistical test for equal variance structure was performed on the data and the results indicated that a quadratic discriminant function is appropriate for the data. The quadratic discriminant function from x to group i is defined as:

$$D_i^2(x) = d_i^2(x) + Ln(|S_i|) - 2Ln(p_i).$$

where $d_i^2(x) = (x - \bar{x}_i)^T S_i^{-1}(x - \bar{x}_i)$, S_i is the within-group covariance matrix for group i, and p_i is the prior probability for group i. The posterior probability of x belonging to group i is then calculated according to Bayes theorem as:

$$P(i|x) = \frac{\exp(-.5D_i^2(x))}{\sum_k \exp(-.5D_k^2(x))}$$

To examine the plot separability, we first applied stepwise discriminant analysis to identify the significant variable(s) suitable for discrimination

among the conditions. Secondly, the discriminant procedure was used to determine the discriminant function of the responses which best describes each condition. Each observation was assigned a probability of belonging to a given group or class based on the distance of its discriminant function from that of each class mean. Variables included in the analysis were estimated LAI, stem density, the percentage of each tree species (live or dead), the total BA, mean height, mean dbh and shortest distance to open flowing water. For the estimated LAI, value 0 for one field plot indicates that it must be a dead plot. Therefore, a total of 9 field plots were first classified to dead based on estimated LAI values for classifications using all data. When only using the data for living trees 3 field plots were classified to the dead class based on estimated LAI values. The discriminant analysis was then applied to the remaining 52 field plots. This analysis requires that the variables have multivariate normal distribution in each of the groups. This assumption was examined using Shapiro–Wilk, Kolmogorov–Smirnov, Cramer-von Mises, and Anderson–Darling methods for each of the variables. When the normal distribution assumption was violated, a Box–Cox transformation was then used to make the distribution of that variable normal.

Field collected data were further classified based on the discriminant function. The purpose of this step was to examine if the model fit the data appropriately, i.e., the model's ability to correctly predict the outcome modeled by the explanatory variables. If the accuracy is high, it would indicate that the model might be adequate for the data. However, the results obtained from discriminant analysis may only be applicable to the sample used. We required a discriminant model which has both external and internal validity and, therefore, cross-validation was also performed to check on the propensity to inflate the accuracy if all data are being used. The classification was performed using the leave-one-out procedure, i.e., each field plot is classified using the discriminant function constructed by taking that plot out of the data set. Hence, each field plot was reclassified as if it were a new unknown observation. Cross-validation provides a better, but more conservative, assessment of classification accuracy.

Results and discussion

Species and field plot data

Based on a previous classification procedure (Kovacs et al. 2008b) and actual field mangrove conditions, all field plot data were grouped into four conditions: tall healthy, dwarf healthy, poor condition, and dead. Tall healthy condition includes mixed mangrove species with most of them tall black mangrove trees that are typically much greater than 2 m height. This mangrove condition appears mainly in the coastal fringe where daily tidal inundation occurs. Poor condition, dwarf and dead mangroves are generally further inland from the water's edge in areas currently flooded only at the highest of tides.

The most dominant mangrove species in this area is the black mangrove having the smallest average dbh and mean height (Tables 1, 2). Black, white, and red mangrove represented 90.12, 8.51 and 1.26% of the total number of trees recorded, respectively (Table 1). However, the values would be 88.84, 9.27, and 1.88% if only live trees were counted. It is also clear that this mangrove forest is undergoing serious degradation (Table 1): among the 10,150 trees measured, about 44% of the trees were dead or cut. In particular, black

Table 1 The number of individual tree species in various conditions

Field plot class	Live			Dead			Cut	Total
	A.g.	*L.r.*	*R.m.*	*A.g.*	*L.r.*	*R.m.*		
Tall healthy	2339	535	121	306	256	10	7	3574
Dwarf healthy	1976	0	0	824	2	0	0	2802
Poor condition	1123	62	0	709	9	0	0	1903
Dead stands	282	0	0	1589	0	0	0	1871
Total	5720	597	121	3428	267	10	7	10150

A.g., Avicennia germinans; L.r., Laguncularia racemosa; R.m., Rhizophora mangle

Table 2 Descriptive statistics of dbh and height for different species (all trees)

Tree type	*n*	dbh (cm) mean (SD)	Height (m) mean (SD)
A.g. (live)	5720	4.63 (2.63)	3.76 (2.90)
L.r. (live)	597	5.21 (1.94)	6.78 (2.66)
R.m. (live)	121	5.40 (3.22)	5.82 (2.09)
A.g. (dead)	3428	6.64 (3.94)	1.81 (1.50)
L.r. (dead)	267	13.37 (9.61)	3.31 (2.85)
R.m. (dead)	10	4.05 (1.25)	2.98 (2.12)
Cut	7	8.36 (3.88)	1.36 (0.48)

A.g., Avicennia germinans; L.r., Laguncularia racemosa; R.m., Rhizophora mangle

Table 3 Descriptive statistics and Shannon–Wiener diversity index (H') for mangrove conditions with all trees included

Condition	Number of plots	H'	LAI mean (std)	Dbh (cm) mean (SD)	Height (m) mean (SD)	Distance to freshwater (m) mean (SD)	Stem density (stems/ha)
Tall healthy	17	1.10	3.98 (.58)	6.43 (4.72)	5.7 (3.1)	56.86 (29.53)	7007
Dwarf healthy	15	0.61	1.96 (.55)	4.07 (1.68)	1.9 (0.8)	137.15 (44.60)	6227
Poor condition	13	0.81	1.53 (.68)	5.62 (3.88)	2.5 (1.7)	159.03 (110.66)	4879
Dead	16	0.42	0.092 (.15)	6.21 (3.3)	1.5 (1.2)	305.95 (239.09)	3898

and white mangroves are undergoing significant degradation, with 24.47 and 30.90% of these trees identified as dead, respectively. Comparatively, red mangrove shows the best condition (Table 1). Currently, the tall red mangrove trees have the largest mean dbh (5.40 cm) and mean height (5.82 m) amongst the three species (Table 2). The red mangrove exists mainly along the fringe closest to the estuaries, and having only 5.47% of its sample identified as dead or cut for timber. The cutting of mangroves, particularly along the fringe is due to the fact that this mangrove forest is not far away from local communities which extract the timber for a variety of purposes (Kovacs 1999). According to the results, white mangrove historically depicted the largest mean dbh and mean heights (based on measurements from dead white mangroves, dbh 13.37 cm, height 3.31 m). Therefore, it is highly plausible that white mangrove has been replaced by red mangrove in the fringe zone. Several very large dead white mangrove trunks still exist in these stands and may be the reason the white mangrove still has the largest average height. This significant change in mangroves might have been caused by changes in hydrology resulting from the canal as suggested by others.

Historical data also show mangrove species diversity is decreasing and the sizes and heights of the trees are becoming smaller and shorter (Tables 3, 4). With regards to species diversity, dbh, and mean height for mangroves with various conditions, tall healthy mangroves recorded the highest values. Poor condition mangroves depict medium diversity, dbh and heights. Dwarf mangroves show the lowest diversity, dbh and heights (Tables 3 and 4). The diversity has decreased over time as is indicated by the decrease of the H' value. For the tall mangroves the H' value dropped from 1.10 (all trees) to 0.63 (living trees) ($P = 0.008$). The same trend was observed for tree diameters, with the mean dbh value decreasing from 6.43 to 5.57 cm ($P < 0.001$). This is mainly due to the fact that the poor condition mangrove currently contains a fair number of large dead trunks as well as some of large trunks that are still alive but in very poor condition. The dwarf mangrove is quite homogeneous, short and typical in appearance to dwarf mangrove found elsewhere. The results of this study are coincidental with the change of species diversity of another mangrove forest in northern Australia (Ball 1998) where species richness was influenced by soil water salinity changes. In that study the maximum diversity was found in areas with moderate salinities (Ball 1998). One interesting observation of this study is that the species diversity of the poor mangrove class is higher than that of dwarf mangrove. This is not surprising given that the dwarf mangroves of this region are quite homogenous and thus lack variation.

Table 4 Descriptive statistics and Shannon–Wiener diversity index (H') for mangrove conditions with only live trees included

Condition	Number of plots	Number of trees	H'	dbh (cm) mean (SD)	Height (m) mean (SD)	Stem density (stems/ha)
Tall healthy	17	2995	0.63	5.57 (3.02)	6.29 (2.97)	5872
Dwarf healthy	15	1976	0	3.71 (1.28)	1.96 (0.76)	4391
Poor condition	13	1185	0.21	4.36 (2.54)	2.62 (1.50)	3038
Dead	10	282	0	3.77 (1.32)	1.61 (0.65)	940

Table 5 Error matrix of classification based on all trees

	Condition classified				Total	User's accuracy (%)
	Tall healthy	Dwarf healthy	Poor condition	Dead		
Tall healthy	17	0	0	0	17	100
Dwarf healthy	0	15	0	0	15	100
Poor condition	0	1	12	0	13	92.3
Dead	0	0	0	16	16	100
Total	17	16	12	16	61	
Producer's accuracy(%)	100	93.75	100	100		

Note: The producer's accuracy is the ratio of the number of field plots that were correctly classified with the actual number of field plots of various conditions. User's accuracy is the ratio of the number of field plots that were correctly classified with total number of field plots that were classified as that class. For both Tables 5 and 6, the 9 Dead classes were first identified using the estimated LAI values and the discriminant analysis was performed on the remaining 52 sampling plots

The discriminant analysis

The analysis was carried out for conditions including all trees and then including only live trees. When all trees are included (total 61 plots), estimated LAI (P-value < 0.0001), mean height (P-value < 0.0001), percentage of dead mangrove (P-value $= 0.0013$), and mean dbh (P-value $= 0.0177$) are found to be significant variables for distinguishing the four classes of mangrove condition. We further tested the appropriateness of using these variables to explain the degradation of mangroves by classifying field plot data. The prior probabilities are set to be proportional to the number of field plots in each class, i.e., 17/52, 15/52, 13/52, and 7/52 for tall healthy, dwarf healthy, poor condition, and dead, respectively. The natural logarithms of the determinant of the covariance matrix ($|S_i|$) are -9.10, -12.44, -6.56, and -13.43 for these four respective classes. Within covariance matrices were then used in the discriminant function since a test of homogeneity of within covariance matrices using Chi-square statistics showed a significant result (P-value < 0.0001). Using this model, the number of observations and percent classified into condition were calculated (Table 5). The model results are very satisfactory in the classification for the conditions with an overall accuracy of 98.4%. There is only one poor condition field plot which was misclassified as dwarf healthy. Using cross-validation, the results indicate that on average 8 of the 61 field plots were misclassified with an overall accuracy of 90.2% (Table 6) which is still satisfactory. The poor condition mangrove plots were misclassified more than any other, with a few field plots classified as dead and dwarf healthy mangroves (Table 6). This result may be expected given the poor condition class is a transitional one.

When only live trees are considered, there are a total of 55 field plots. Three plots with estimated LAI values of 0 were identified and assigned to the dead class. The discriminant analysis was then performed on the remaining 52 field plots. The significant variables of this model are the estimated LAI, the mean height, and the mean dbh (P-value < 0.0001). With proportional prior probabilities and within covariance matrices, the number of observations and percent classified into condition are given in Table 7. The overall accuracy of classification is 92.7%. There

Table 6 Error matrix of classification using cross-validation based on all trees

	Condition classified				Total	User's accuracy (%)
	Tall healthy	Dwarf healthy	Poor condition	Dead		
Tall healthy	16	0	1	0	17	94.1
Dwarf healthy	0	13	2	0	15	86.7
Poor condition	0	1	12	0	13	92.3
Dead	0	0	2	14	16	87.5
Total	16	14	17	14	61	
Producer's accuracy(%)	100	92.9	70.6	100		

Table 7 Error matrix of classification based on live trees only

Note: For both Tables 7 and 8, the 3 Dead classes were first identified using the estimated LAI values and the discriminant analysis was performed on the remaining 52 field sampling plots

	Condition classified				Total	User's accuracy (%)
	Tall healthy	Dwarf healthy	Poor condition	Dead		
Tall healthy	17	0	0	0	17	100
Dwarf healthy	0	15	0	0	15	100
Poor condition	0	4	9	0	13	69.2
Dead	0	0	0	10	10	100
Total	17	19	9	10	55	
Producer's accuracy(%)	100	78.9	100	100		

Table 8 Error matrix of classification using cross-validation for live trees only

	Condition classified				Total	User's accuracy (%)
	Tall healthy	Dwarf healthy	Poor condition	Dead		
Tall healthy	16	0	1	0	17	94.1
Dwarf healthy	0	13	2	0	15	86.7
Poor condition	0	5	8	0	13	61.5
Dead	0	0	2	8	10	80
Total	16	18	13	8	55	
Producer's accuracy (%)	100	72.2	61.5	100		

are four dwarf healthy plots which are misclassified as poor condition. Using cross-validation, the results show that on average 10 of the 55 field plots were misclassified with an overall accuracy of 81.8% (Table 8). Although a lower accuracy was achieved, the results are similar to the one based on all trees. The results also show the large variations in poor condition mangrove plots and the similarity between dwarf and poor condition mangroves. The observed drop of the classification accuracy based on live trees is mainly due to the confusion of these two classes.

Furthermore, estimated LAI, an indicator of mangrove structure and productivity, is an important variable in regards to mangrove condition. If excluded from analysis the overall accuracies, based on all trees, drop from 98.4 and 90.2% to 95.1 and 86.9% in the classification and validation procedures, respectively. There are also misclassifications between tall healthy and poor condition field plots if the LAI variable is excluded (data not shown). Other variables, i.e., mean height and dbh, were also found to be significant for classification. These results show environmental change has shaped the mangroves to such a degree that it is possible to classify them based on these biological variables. The high accuracies of the field plot classifications and the cross-validation

procedures also suggest it is logically reasonable and feasible to classify the mangroves of the Isla La Palma into the four classes previously employed by others. These classes should not only be considered in further satellite image classification procedures but also used in any further field studies for these mangroves. It is safe to conclude from the results of these field data analyses that the four mangrove classes previously employed for satellite image classification are appropriate for this study area.

Conclusion

The results of this study do indicate that, based on field plot data, the mangroves of this system have experienced considerable degradation. The mean height, mean dbh, and species diversity values of the mangroves under investigation have all decreased considerable when examining all trees together or when only considering live trees. It is also apparent from the results that the most dominant species within this study area, the black mangrove (*Avicennia germinans*), has been particularly affected. Most importantly, the statistical procedure used on the field plot data would suggest that the classification scheme previously employed for mapping the condition of the mangroves in this study area is in fact appropriate. Specifically, the categorization of mangroves as either tall healthy, dwarf healthy, poor condition or dead is representative for the Isla La Palma region. The results of the stepwise discriminant analysis procedure would also suggest that the estimated LAI, mean height, and mean dbh are the most significant variables in the classification of the mangroves for this region. In conclusion, it is suggested that the techniques applied to the mangrove field plot data in this study not only provide justification for the use of the four class mangrove classification scheme in mapping mangroves from remotely sensed data, but also may provide insight to the environmental variables most influential to the current structure of these forests. The results of this investigation also support the postulation that changes in the hydrological regime following the opening of the Cuautla canal may have contributed to the observed degradation of this mangrove forest.

Acknowledgments This study was funded by a Natural Sciences and Engineering Research Council of Canada grant (No. #249496-06) awarded to John M. Kovacs. The authors would like to acknowledge the assistance of Lance P. Aspden and Joshua M.L. King for their assistance in the field data collection campaigns of 2007 and 2008, respectively. We appreciate the comments from the anonymous reviewers which helped improve the quality of this paper.

References

Allen J, Ewel AK, Jack J (2001) Patterns of natural and anthropogenic disturbance of the mangroves on the Pacific Island of Kosrae. Wetlands Ecol Manage 9:279–289

Ball MC (1998) Mangrove species richness in relation to salinity and waterlogging: a case study along the Adelaide River floodplain, Northern Australia. Glob Ecol Biogeogr Lett 7:73–82

Barbier EB, Sathirathai S (2004) Shrimp farming and mangrove loss in Thailand. Edward Elgar, London

Basak UC, Das AB, Das P (1996) Chlorophylls, carotenoids, proteins and secondary metabolites in leaves of 14 species of mangroves. Bull Marine Sci 58:654–659

Berlanga-Robles CA, Ruiz-Luna A (2002) Land use mapping and change detection in the coastal zone of Northwest Mexico using remote sensing techniques. J Coastal Res 18:514–522

Cole TG, Ewel KC, Devoe NN (1999) Structure of mangrove trees and forests in Micronesia. Forest Ecol Manage 117:95–109

Duke NC, Meynecke JO, Dittmann S, Ellison AM, Anger K, Berger U, Cannicci S, Diele K, Ewel KC, Field CD, Koedam N, Lee SY, Marchand C, Nordhaus I, Dahdouh-Guebas F (2007) A world without mangroves? Science 317:41–42

Green EP, Clark CD, Mumby PJ, Edwards AJ, Ellis AC (1998) Remote sensing techniques for mangrove mapping. Int J Remote Sens 19:935–956

Everitt JH, Yang C, Judd FW (2010) Use of archive aerial photography for monitoring black mangrove populations. J Coastal Res 26:649–653

Ewel KC, Twilley RR, Ong JE (1998) Different kinds of mangrove forests provide different goods and services. Glob Ecol Biogeogr Lett 7:83–94

Flores-Verdugo FJ, Gonzáles-Farías F, Blanco-Correa M, Nuñez-Pastén A (1997) The Teacapan-Agua Brava-Marismas Nacionales mangrove ecosystem on the Pacific coast of Mexico. In: Kjerve B, Drude de Lacerda L, Diop EHS (eds) Mangrove ecosystem studies in Latin America and Africa. UNESCO,ISME & US Forest Service, US, pp 35–46

Fuente G, Carrera E (2005) Cambio de uso del suelo en la zona costera del Estado de Sinaloa. Final report to United States Forest Service. Grant no. 03-DG-11132762-157, Mexico: Ducks Unlimited de Mexico, AC, Garza Garcia, NL

Held A, Ticehurst C, Lymburner L, Williams N (2003) High resolution mapping of tropical mangrove ecosystems using hyperspectral and radar remote sensing. Int J Remote Sens 24:2739–2759

Hirano A, Madden M, Welch R (2003) Hyperspectral image data for mapping wetland vegetation. Wetlands 23:436–448

Hogarth PJ (1999) The biology of mangroves. Oxford University Press, Oxford
Kovacs JM (1999) Assessing mangrove use at the local scale. Landscape Urban Plan 43:201–208
Kovacs JM (2000) Perceptions of environmental change in a tropical coastal wetland. Land Degrad Dev 11:209–220
Kovacs JM, Wang J, Blanco-Correa M (2001) Mapping mangrove disturbances using multi-date Landsat TM imagery. Environ Manage 27:763–776
Kovacs JM, Flores-Verdugo F, Wang J, Aspden LP (2004) Estimating leaf area index of a degraded mangrove forest using high spatial resolution satellite imagery. Aquat Bot 80:13–22
Kovacs JM, Wang J, Flores-Verdugo F (2005) Mapping mangrove leaf area index at the species level using IKONOS and LAI-2000 sensors for the Agua Brava Lagoon, Mexican Pacific. Estuarine Coastal Shelf Sci 62:377–384
Kovacs JM, Vandenberg CV, Flores-Verdugo F (2006) Assessing fine beam RADARSAT-1 backscatter from a white mangrove (*Laguncularia racemosa* (Gaertner)) canopy. Wetlands Ecol Manage 14:401–408
Kovacs JM, Vandenberg CV, Wang J, Flores-Verdugo F (2008a) The use of multipolarized spaceborne SAR backscatter for monitoring the health of a degraded mangrove forest. J Coastal Res 24:248–254
Kovacs JM, Zhang C, Flores-Verdugo F (2008b) Mapping coastal wetland using C-band ENVISAT ASAR and landsat optical data. Cienc Marinas 34:407–418
Kovacs JM, King JML, Flores de Santiago F, Flores-Verdugo F (2009) Evaluating the condition of a mangrove forest of the Mexican Pacific based on an estimated leaf area index mapping approach. Environ Monit Assess 157:137–149
Krause G, Bock M, Weiers S, Braun G (2004) Mapping landcover and mangrove structures with remote sensing techniques— a contribution to a synoptic GIS in support of coastal management in North Brazil. Environ Manage 34:429–440
Krebs C (1989) Ecological methodology. HarperCollins, New York
Linneweber V, de Lacerda LD (2002) Mangrove ecosystems: function and management. Springer, Berlin
Long BG, Skews TD (1996) A technique for mapping mangroves with Landsat TM satellite data and geographic information system. Estuarine Coastal Shelf Sci 43:373–381
Lucas RM, Mitchell AL, Rosenqvist A, Proisy C, Melius A, Ticehurst C (2007) The potential of L-band SAR for quantifying mangrove characteristics and change: case studies from the tropics. Aquat Conserv 17:245–264
Madden M, Jones D, Vilcheck L (1999) Photointerpretation key for the everglades vegetation classification system. Photogramm Eng Remote Sens 65:171–177
McDonald KO, Webber DF, Webber MK (2003) Mangrove forest structure under varying environmental conditions. Bull Marine Sci 73:491–505
Mitsch WJ, Gosselink JG (2007) Wetlands. Wiley, New York
Rakotomavo A, Fromard F (2010) Dynamics of mangrove forests in the Mangoky River delta, Madagascar, under the influence of natural and human factors. Forest Ecol Manage 259:1161–1169
Saito H, Bellan MF, Al-Habshi A, Aizpuru M, Blasco F (2003) Mangrove research and coastal ecosystem studies with SPOT-4 HRVIR and TERRA ASTER in the Arabian Gulf. Int J Remote Sens 24:4073–7092
Salovaara KJ, Thessler S, Malik RN, Tuomisto H (2005) Classification of amazonian primary rain forest vegetation using Landsat ETM+ satellite imagery. Remote Sens Environ 97:39–51
Simard M, De Grandi G, Saatchi S, Mayaux P (2002) Mapping tropical coastal vegetation using JERS-1 and ERS-1 radar data with a decision tree classifier. Int J Remote Sens 23:1461–1474
Tong PHS, Auda Y, Populus J, Aizpuru M, Blasco F (2004) Assessment from space of mangrove evolution in the Mekong Delta, in relation to extensive shrimp farming. Int J Remote Sens 25:4795–4812
Vaiphasa C, Ongsomwang S, Vaiphasa T, Skidmore AK (2005) Tropical mangrove species discrimination using hyperspectral data: a laboratory study. Estuarine Coastal Shelf Sci 65:371–379
Valiela I, Boen JL, York JK (2001) Mangrove forests: one of the world's threatened major tropical environments. Bioscience 51:807–815
Walters BB, Ronnback P, Kovacs JM, Crona B, Hussain SA, Badola R, Primavera JH, Barbier E, Dahdouh-Guebas F (2008) Ethnobiology, socio-economics and management of mangrove forests: a review. Aqua Bot 89:220–236
Wang L, Sousa W (2009) Distinguishing mangrove species with laboratory measurements of hyperspectral leaf reflectance. Int J Remote Sens 30:1267–1281
Wang L, Sousa WP, Gong P, Biging GS (2004) Comparison of IKONOS and QuickBird images for mapping mangrove species on the Caribbean coast of Panama. Remote Sens Environ 91:432–440
Wang L, Silvan J, Sousa W (2008) Neural network classification of mangrove species from multiseasonal IKONOS imagery. Photogramm Eng Remote Sens 74:921–927
Welch RW, Madden M, Doren R (1999) Mapping the everglades. Photogramm Eng Remote Sens 65:163–170
Wilkie ML, Fortuna S (2003) Status and trends in mangrove area extent worldwide. http://www.fao.org/docrep/007/j1533e/j1533e00.htm. Accessed 20 april 2009
Xue C (1996) Coastal sedimentation, erosion and management of Kosrae, Federated States of Micronesia. SOPAC Technical Report 228, South Pacific Geoscience Commission, Suva, Fiji
Yu B, Ostland IM, Gong P, Pu RL (1999) Penalized discriminant analysis of in situ hyperspectral data for conifer specie recognition. IEEE Trans Geosci Remote Sens 5:2569–3577